removal seemed to result in a resection with positive or close margins. In this study, the role and significance of postoperative HDRBT alone in the management of STS is analyzed retrospectively.

Methods and materials

From 1995 to 2008, 25 patients with 26 STS lesions underwent postoperative HDRBT alone in National Cancer Center Hospital. There were 10 men and 15 women. In a male patient with malignant fibrous histiocytoma, the lesion was managed with operation and postoperative HDRBT and the tumor recurred proximal to the original site. The recurred tumor was resected and postoperative HDRBT was administered repeatedly (Table 1). Median age was 60.7 years ranging from 9 to 76 years. Primary sites of the tumors were upper extremity with 12 lesions and lower extremity with 11 lesions. Primary truncal STS was seen in three lesions. As for pathology, malignant fibrous histiocytoma was most frequently seen in 12 lesions followed by leiomyosarcoma in three lesions. Eighty-eight percent of lesions were diagnosed as Grade 2 or 3 in three-tiered grade classification. Surgical margins were microscopically positive for sarcoma cells in 13 lesions; whereas in 13 lesions, resection margins were very close (less than 5 mm) to the tumor because vicinity of the tumor to the functionally important structures, such as major neurovascular bundles, made it difficult to attain adequate surgical margins. The maximal tumor size in the pathologic specimen was 9 cm in a mean with a range between 1.2 cm and 22 cm. Included in the present study were also the STSs, which recurred after previous surgeries. Fourteen lesions were treated by resections and HDRBTs for recurrences after the previous surgeries. Number of the foregoing surgeries ranged from one to eight.

Table 1
Age and sex of the 25 patients and characteristics of the 26 lesions undergoing postoperative high–dose rate brachytherapy for soft tissue sarcomas

Characteristics	Number
Median age (y)	60.7 (range, 9–76)
Sex	
Male:female	11:15
Primary Site	
Upper extremity	12
Lower extremity	11
Trunk	3
Histopathology	
Malignant fibrous histiocytoma	12
Leiomyosarcoma	3
Synovial sarcoma	3
Liposarcoma	2
Rhabdomyosarcoma	2
Others	4
Malignant grade	
1	2
2	9
3	15
Tumor size	
Mean	9 cm (range, 1.2–22)
<5 cm	9
>5 cm	17
Number of previous operations	
0	12
>1	14
Status of surgical margin	
Positive	13
Negative	13
Chemotherapy	
Yes	12
No	14

Indication of the postoperative HDRBT was determined preoperatively by a joint meeting of orthopedic surgeons and radiation oncologists. Postoperative HDRBT was used to preserve major neurovascular bundles or major muscles, which are indispensable to maintain the functional integrity of extremities. During the operation, resection margins close to or contaminated by tumor were confirmed by both orthopedic surgeons and radiation oncologists. Surgical clips were placed to delineate the tumor bed as well as the resection margins very close to the lesion. The flexible applicator tubes of HDRBT were placed to cover the tumor bed with 1–2 cm margins in a parallel fashion with 1–1.5 cm intervals between the tubes. Applicator tubes have a closed end and were sutured to the tumor bed. The open ends of tubes were pulled through the skin and connected to the remote afterloading machine. Muscular or adipose tissue flaps of about 5 mm thickness were used to cover major nerve and/or vascular bundles to avoid direct contact of the applicators. The tubes were removed after completion of the HDRBT. Radiation therapy planning was performed by Plato (version 14.3.7; Nucletron, Veenendaal, The Netherlands). The coordinates of the tube applicators were digitized using orthogonal x-rays and/or CT images. The dwell positions of HDRBT source were located to cover tumor bed encircled by the surgical clips. No special efforts were exerted to include all the scar and drainage sites. Geometric optimization was used to calculate dwell times with a reference poinof 5 mm lateral to the midportion of the central tube applicator. For HDRBT, ^{192}Ir afterloading machine was used (microSelectron HDR; Nucletron, Veenendaal, The Netherlands). All the lesions but one were irradiated with a fractional dose of 6 Gy, and the remaining one was treated by 4.5 Gy because neighboring nerve could not be adequately protected by the flap. The HDRBT was done b.i.d. with an interval between the fractions of at least 6 h. Six fractions were administered in all but one lesion, which was treated with four fractions because of the accidental early slip out of the applicators. In 24 lesions, applied dose was 36 Gy, 30 Gy, and 27 Gy each in one lesion (Table 2). Interval

Table 2
Postoperative high–dose rate brachytherapy for soft tissue sarcomas

Characteristics	Number
Interval between OP and BT (days)	
Mean	5.3 (range, 1–7)
<5	2
>5	24
Median number of applicators	7 (range, 2–15)
Fractional dose	
4.5 Gy	1
6 Gy	25
Number of fractions	
5	1
6	25
Total dose (EQD2 for tumor control)	
27 Gy (32.6 Gy)	1
30 Gy (40 Gy)	1
36 Gy (48 Gy)	24
Mean volume encircled by the prescribed dose	74.9 cc (range, 18.5–173)

OP = operation; BT = brachytherapy; EQD2 = equivalent dose with 2 Gy fraction.

between the operation and the HDRBT was 5.3 days in a mean, and 24 HDRBTs were commenced between 5 and 7 days after the operation. Number of implanted tube applicators ranged from two to 15 with a median of seven. The treated volume encircled by the prescribed dose ranged from 18.5 to 173 cc with a mean of 74.9 cc. Chemotherapy was delivered in 12 lesions.

Median followup length was 49.7 months ranging from 4.7 to 187 months. Local recurrence-free survival (LRFS) was calculated in the 26 lesions, and overall survival (OS) in all the 25 patients. Local recurrence was defined as a regrowth of the STS within 5 cm from the operation scars. LRFS and OS were calculated by Kaplan–Meier method (11) with a difference between the survival curves evaluated by a logrank test. Acute morbidities seen within 6 months after HDRBT were classified according to the National Cancer Institute Common Terminology Criteria for Adverse Events version 3.0, whereas Radiation Therapy Oncology Group/European Organization for Research and Treatment for Cancer criteria were used for late morbidities (12).

Results

Local recurrence was observed in five lesions. All the local recurrences occurred outside of the treated volume of HDRBT. These local recurrences were within the treated volume, if postoperative EBRT were administered encompassing all the surgical scars with 5 cm margins. LRFS of all 26 lesions was 78.2% in 5 years. According to the surgical margin status, 5-year LRFSs of positive and negative margins were 90.9% and 64.6%, respectively, without

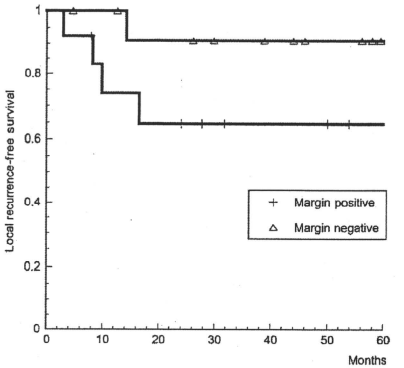

Fig. 1. Local recurrence-free survivals according to surgical margin status.

a statistically significant difference ($p = 0.11$) (Fig. 1). In the lesions treated as a primary therapy, LRFS is 90.9% in 5 years, whereas the recurrent lesions after previous operations showed 5-year LRFS rate of 66.5% ($p = 0.15$) (Fig. 2). The lesions were classified into two groups according to the surgical margin status and number of foregoing operations. Group 1 was defined as recurrent lesions, which were resected with positive surgical margins. All other lesions were classified into Group 2. There were eight lesions in Group 1 and 18 in Group 2. Five-year LRFS was 43.8% and 93.3% in Group 1 and Group 2, respectively

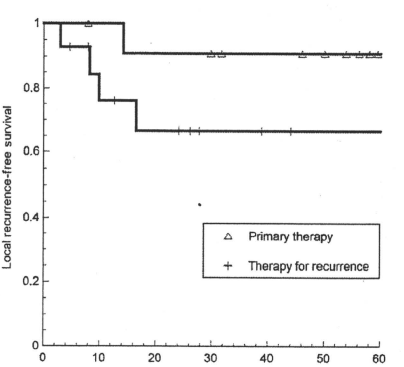

Fig. 2. Local recurrence-free survivals according to number of previous operations.

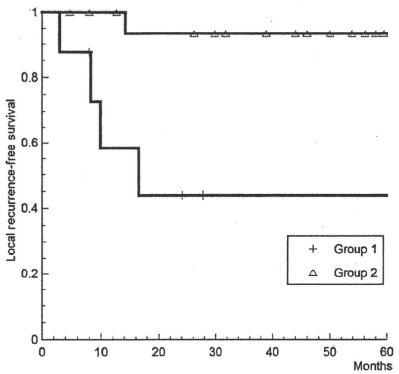

Fig. 3. Local recurrence-free survivals according to the group classification by surgical margin status and number of previous operations (for details refer to the text).

(Fig. 3). The difference reached a statistical significance with $p = 0.004$. Sex, malignant grade, tumor size, number of applicators, and treated volume were found to have no statistically significant influences on LRFS. In the 23 lesions of the extremity STSs, only one amputation was required to control recurrence.

OS of 25 patients was 75.6% in 5 years. There were only 2 patients with Grade 1 malignancy and both of them were alive without recurrence. The patients with Grade 2 and 3 lesions showed similar OSs and 71.6% of them were alive for 5 years.

Acute morbidities were seen in 7 patients with Grade 1 morbidities in 6 patients and Grade 2 in 1 patient (Table 3). Grade 1 morbidities were a slight bleeding from the scar at the time of applicator removal, slight erosion of skin, and seroma formation requiring aspiration only once or twice. Grade 2 morbidity was wound dehiscence, which healed with conservative measures. Chronic morbidities were seen in 4 patients. The Grade 3 and 4 morbidity were seen each in 1 patient. Grade 4 morbidity was bone exposure at the HDRBT site requiring surgical removal of the sequester and repair with bone transplantation. The Grade 3 morbidity was fistula formation with an ensuing infection managed by debridement. Both morbidities occurred within 24 months after HDRBT. Five-year rate of chronic morbidities equal to or greater than Grade 2 was 14.6%.

Table 3
Number of morbidities of postoperative high–dose rate brachytherapy

Morbidities	Morbidity grade	Number of morbidities
Acute morbidity		
Wound complication	1	4
	2	2
Paresthesia	1	1
Seroma formation	1	1
Late morbidity		
Wound complication	2	1
Seroma formation	1	1
Bone exposure	4	1
Infectious fistula	3	1

Discussions

In the management of STS, limb-sparing operation with perioperative radiation therapy has been established as a standard (13). With that combination, LRFS rate is reported to be 75–100% (1–4, 14). However, local recurrence rate is strongly influenced by the surgical margin status, number of previous operations, grade of malignancy, and primary site of STS (1, 2). In the present study, operative margins were microscopically positive in 50% of the patients and the remaining patients had very close margins less than 5 mm. Furthermore, 54% of the lesions were classified as Grade 3 malignancies. Considering the adverse features of this series, LRFS rate of 78.2% in 5 years is relatively favorable. The marginal status, number of the previous operations, and the grade of malignancy did not have an influence on LRFS with a statistical significance, probably because of the small number of the patients in this series. However, the recurrent lesions resected with positive surgical margins showed a poor 5-year LRFS of 43.8% in comparison to the other lesions with 93.3% LRFS in 5 years.

Brachytherapy has an advantage of concentrating dose distribution onto the tumor region with a simultaneous sparing of normal tissues (15), whereas EBRT with wide fields encompassing tumor as well as surgical beds sometimes causes bone fracture, subcutaneous fibrosis, and lymphedema distal to the irradiated site (16). According to Memorial Sloan-Kettering Cancer Center studies, postoperative LDRBT as a single modality reduces local recurrence in margin-negative high-grade STS (1, 3). The LDRBT did not include operative scars and drainage scars in the treated volume. In contrary, local recurrence was not reduced by LDRBT alone in postoperative low-grade STSs (17). They also suggested that high-grade STSs with positive surgical margins are better treated by combination of EBRT and LDRBT (5). Although HDRBT has advantages that radiation dose distribution can be optimized by the manipulation of dwell positions and dwell times of ^{192}Ir source, and radiation exposure to the medical personnel is negligible, the paucity of reported series makes it difficult to establish the optimal fractionation and total dose of HDRBT (6–10). Retrospective analyses revealed that combined EBRT and HDRBT is well tolerated and reduce local recurrence. Chun *et al.* (6) showed that local recurrence was not seen in 17 patients treated with 12–18 Gy

of 6 fractions of HDRBT combined with EBRT of 36–60 Gy. Pohar *et al.* (9) demonstrated that 2-year local control of 94% could be obtained with HDRBT of 13.5 Gy in three fractions with EBRT. Koizumi *et al.* (7) showed somehow poorer local control rate of 48% in 2 years because of the adverse features of their patients with macroscopic residual disease in 31%. In the present study, HDRBT was used without EBRT. HDRBT was delivered to the tumor bed without including surgical and drainage scars. At the launch of the postoperative HDRBT, radiation was planned to be confined to the tumor bed based on the reports from Memorial Sloan-Kettering Cancer Center. Because most of the patients in this series underwent resections reaching to the major neurovascular bundles and the high-dose radiation to them could cause serious morbidities, the total dose of HDRBT was determined by tolerance dose of peripheral nerve assumed as about 60 Gy in a conventional fractionation. The corresponding biologically equivalent dose by 2 Gy fractionation was calculated by linear quadratic model assuming $\alpha/\beta = 10$ Gy and 3 Gy for tumor control and late toxicity, including nerve damage, respectively (18). The equivalent dose by 2 Gy fractionation for HDRBT of 36 Gy was 48 Gy and 64.8 Gy, respectively, for tumor control and late toxicity. Because of the favorable results, this field setup and fractionation regimen of HDRBT have been continued to the present time.

Despite the retrospective nature of this study and the small number of patients, HDRBT alone with the fractionation regimens used in this study seems to be satisfactory to sterilize lesions in the treated volume. However, poor LRFS of 43.8% in 5 years demonstrates that in lesions treated for recurrence and whose surgical margins are positive, STSs tended to recur outside of the treated volume of HDRBT but within 5 cm from the surgical scars. It seems that they had better been treated with combination of HDRBT and wide field EBRT encompassing surgical beds as well as scars and drainage sites.

Serious late morbidity was seen in 2 patients, both of which could be repaired by surgical procedures. Although it is recommended to begin brachytherapy no sooner than 5 days after the operation (1, 15), 2 patients irradiated with a shorter interval did not have any serious morbidities. There were no patients who underwent limb amputation because of morbidities.

Conclusions

In summary, HDRBT alone to the tumor bed without including surgical scars and drainage sites with 36 Gy/6 fractions/3 d seems to be adequate and tolerable as a postoperative treatment for patients initially operated and/or negative for surgical margins. If the lesion is operated for recurrence and surgical margins are positive, administration of wide fields EBRT is recommended.

Acknowledgment

This work was partly supported by Grant-in-Aid for Cancer Research from the Ministry of Health, Labor, and Welfare, Japan.

References

[1] Pisters PWT, Leung DHY, Woodruff J, *et al.* Analysis of prognostic factors in 1041 patients with localized soft tissue sarcomas of the extremities. *J Clin Oncol* 1996;14:1679–1689.

[2] Zagars GK, Ballo MT, Pisters PWT, *et al.* Preoperative vs. postoperative radiation therapy for soft tissue sarcoma: A retrospective comparative evaluation of disease outcome. *Int J Radiat Oncol Biol Phys* 2003;56:482–488.

[3] Pisters PWT, Harrison LB, Leung DHY, *et al.* Long-term results of a prospective randomized trial of adjuvant brachytherapy in soft tissue sarcoma. *J Clin Oncol* 1996;14:859–868.

[4] Yang JC, Chang AE, Baker AR, *et al.* Randomized prospective study of the benefit of adjuvant radiation therapy in the treatment of soft tissue sarcomas of the extremity. *J Clin Oncol* 1998;16:197–203.

[5] Alekhteyar KM, Leung DH, Brennan MF, *et al.* The effect of combined external beam radiotherapy and brachytherapy on local control and wound complications in patients with high-grade soft tissue sarcomas of the extremity with positive microscopic margin. *Int J Radiat Oncol Biol Phys* 1996;36:321–324.

[6] Chun M, Kang S, Kim BS, *et al.* High dose rate interstitial brachytherapy in soft tissue sarcoma: Technical aspects and results. *Jpn J Clin Oncol* 2001;31:279–283.

[7] Koizumi M, Inoue T, Yamazaki H, *et al.* Perioperative fractionated high-dose rate brachytherapy for malignant bone and soft tissue tumors. *Int J Radiat Oncol Biol Phys* 1999;43:989–993.

[8] Martinez-Monge R, San Julian M, Amillo S, *et al.* Perioperative high-dose-rate brachytherapy in soft tissue sarcomas of the extremity and superficial trunk in adults: Initial results of a pilot study. *Brachytherapy* 2005;4:264–270.

[9] Pohar S, Haq R, Liu L, *et al.* Adjuvant high-dose-rate and low-dose-rate brachytherapy with external beam radiation in soft tissue sarcoma: A comparison of outcomes. *Brachytherapy* 2007;6:53–57.

[10] Nag S, Porter AT, Donath D. The role of high dose rate brachytherapy in the management of adult soft tissue sarcomas. In: Nag S, editor. *High dose rate brachytherapy. A textbook.* New York, NY: Futura Publishing Company; 1994. p. 393–408.

[11] Kaplan EL, Meier P. Nonparametric estimation from incomplete observations. *J Am Stat Assoc* 1958;53:457–481.

[12] Perez CA, Brady LW. Principles and practice of radiation oncology. Philadelphia, PA: JB Lippincot Company; 1993. pp. 53–55.

[13] Pisters PWT, O'Sullivan B, Maki RG. Evidence-based recommendations for local therapy for soft tissue sarcomas. *J Clin Oncol* 2007;25:1003–1008.

[14] Suit HD, Mankin HJ, Wood WC, *et al.* Treatment of the patient with stage M0 soft tissue sarcoma. *J Clin Oncol* 1988;6:854–862.

[15] Nag S, Shasha D, Janjan N, *et al.*, American Brachytherapy Society. The American Brachytherapy Society recommendations for brachytherapy of soft tissue sarcomas. *Int J Radiat Oncol Biol Phys* 2001;49:1033–1043.

[16] Davis AM, O'Sullivan B, Turcotte R, *et al.*, Canadian Sarcoma GroupNCI Canada Clinical Trial Group Randomized Trial. Late radiation morbidity following randomization to preoperative versus postoperative radiotherapy in extremity soft tissue sarcoma. *Radiother Oncol* 2005;75:48–53.

[17] Pisters PWT, Harrison LB, Woodruff JM, *et al.* A prospective randomized trial of adjuvant brachytherapy in the management of low-grade soft tissue sarcomas of the extremity and superficial trunk. *J Clin Oncol* 1994;12:1150–1155.

[18] Fowler JF. The linear-quadratic formula and progress in fractionated radiotherapy. *Br J Radiol* 1989;62:679–694.

Int. J. Radiation Oncology Biol. Phys., Vol. 77, No. 4, pp. 1017–1023, 2010

0360-3016/$–see front matter

ELSEVIER

doi:10.1016/j.ijrobp.2009.06.066

CLINICAL INVESTIGATION **Head and Neck**

OUTCOMES IN PATIENTS WITH EARLY-STAGE HYPOPHARYNGEAL CANCER TREATED WITH RADIOTHERAPY

RYO-ICHI YOSHIMURA, M.D.,*† YOSHIKAZU KAGAMI, M.D.,* YOSHINORI ITO, M.D.,* MASAO ASAI, M.D.,‡ HIROSHI MAYAHARA, M.D.,* MINAKO SUMI, M.D.,* AND JUN ITAMI, M.D.*

Division of *Radiation Oncology and ‡Head and Neck Surgery, National Cancer Center Hospital, and †Department of Diagnostic Radiology and Oncology, Head and Neck Reconstruction Division, Graduate School, Tokyo Medical and Dental University, Tokyo, Japan

Purpose: To analyze the outcome in patients with early-stage hypopharyngeal cancer (HPC) who were treated with radiotherapy (RT).

Methods and Materials: Between February 1988 and February 2007, 77 patients with Stage I or Stage II HPC underwent definitive RT in the Division of Radiation Oncology at the National Cancer Center Hospital. Eleven of the patients received local irradiation, and the other 66 patients received elective bilateral neck irradiation and booster irradiation to the primary lesion. The median follow-up period for all the patients was 33 months from the start of RT, ranging from 3 to 229 months.

Results: The rates of overall survival, HPC-specific survival, HPC recurrence-free survival, and local control with laryngeal voice preservation for the 77 patients at 5 years were 47%, 74%, 57%, and 70%, respectively. The survival rates were not affected by the patient characteristics or treatment factors, but the RT field was significantly correlated with local control in a multivariate analysis. Seven of the patients had Grade 3 or greater complications, but these complications occurred after salvage surgery in 6 of the patients. Of the 77 patients, 83% had synchronous or metachronous malignancies, but these malignancies did not influence the survival of the patients if the malignancies were detected at an early stage.

Conclusion: RT is an appropriate treatment method for early-stage HPC. However, because synchronous or metachronous malignancies occur at a relatively high frequency, careful follow-up and the early detection of such malignancies are critical. © **2010 Elsevier Inc.**

Hypopharyngeal cancer, Radiotherapy, Synchronous malignancy, Metachronous malignancy.

INTRODUCTION

Patients with hypopharyngeal cancer (HPC) are often first diagnosed at an advanced stage. Because the diagnosis of early-stage HPC is relatively rare, few reports have analyzed the treatment results of early-stage HPC; thus, the optimal treatment for this condition remains uncertain (1).

Foote (2) reported that treatment options for early-stage HPC included endoscopic removal, open function-sparing partial laryngopharyngectomy, total laryngectomy with partial pharyngectomy, and radiotherapy (RT); factors in treatment selection were reported to be the extent and volume of the tumor (including anterior commissure involvement), patient preference (including occupational considerations), patient age, comorbid illnesses, patient compliance, voice quality, physician experience and skill, previous head-and-neck malignancy, risk of a second head-and-neck primary cancer, treatment cost, and physician and institutional biases.

At the National Cancer Center Hospital, patients with Stage I or II HPC are often treated with RT alone. In this study, we reviewed the data on patients who were treated with RT for early-stage HPC and analyzed the outcomes in these patients.

METHODS AND MATERIALS

Patient characteristics

Between February 1988 and February 2007, 77 patients with Stage I (T1N0M0) or Stage II (T2N0M0) HPC underwent RT in the Division of Radiation Oncology at the National Cancer Center Hospital. These patients consisted of 6 women and 71 men, ranging in age from 42 to 80 years (median, 63 years) (Table 1). All the tumors were diagnosed as squamous cell carcinoma by histopathologic examination of the biopsy specimens, and each tumor was staged retrospectively according to the 2002 UICC TNM classification system based on a complete patient history and physical

Reprint requests to: Ryo-ichi Yoshimura, M.D., Department of Diagnostic Radiology and Oncology, Head and Neck Reconstruction Division, Graduate School, Tokyo Medical and Dental University, 1-5-45, Yushima Bunkyo-ku, Tokyo 113-8519, Japan. Tel: +81) 3-5803-5311; Fax: (+81) 3-5803-0147; E-mail: ysmrmrad@tmd.ac.jp

Conflict of interest: none.

Received Jan 13, 2009, and in revised form May 10, 2009. Accepted for publication June 12, 2009.

Table 1. Patient characteristics

Characteristic	Stage I (n = 42)	Stage II (n = 35)
Sex		
F	2	4
M	40	31
Age (y)		
Range (median)	42–80 (63)	48–79 (63)
HPC site		
Postcricoid region	6	6
Pyriform fossa	30	20
Posterior wall	6	9
Radiotherapy field and dose		
Local	6	5
Dose range (median) (Gy)	60–66 (60)	60–70 (61)
Locoregional	36	30
Primary dose range (median) (Gy)	58–70 (66)	60–70 (66)
Subclinical dose range (median) (Gy)	32–46 (40)	20–50 (40)
Concurrent chemotherapy		
CDDP + 5-FU	10	5
TS-1	1	0

Abbreviations: HPC = hypopharyngeal cancer; CDDP = cisplatin; 5-FU = 5-fluorouracil; TS-1 = tegafur-gimeracil-oteracil potassium.

examination record. The primary sites were the pyriform fossa (PS) in 50 patients (65%), the posterior wall (PW) in 15 (19%), and the postcricoid region (PC) in 12 (16%). At the time when the HPC was found, 21 patients (27%) had symptoms: 12 patients experienced pain in their pharynx, 9 experienced discomfort in their pharynx, and 1 patient experienced a change in his voice (hemilarynx fixation was not observed). Fifty-two patients (68%) were asymptomatic; their HPCs were found by gastrointestinal endoscopy performed as part of a follow-up examination for metachronous malignancies treated before to the diagnosis of HPC in 38 patients (49%: esophageal cancer in 31, gastric cancer in 2, oropharyngeal cancer in 2, oral cancer in 2, and esophageal and gastric cancer in 1), an examination performed before the treatment of some other disease in 10 patients (13%: esophageal cancer in 7, oral cancer in 1, gastric ulcer in 1, and pneumonia in 1), and as part of a general health examination in 4 patients. The symptoms of the remaining 3 patients were not documented.

Treatment

All the patients underwent definitive RT. Either a 4-MV or a 6-MV linac X-ray was used to administer a daily dose of 2 Gy 5 days a week, with a total dosage of 58–70 Gy (median, 66 Gy). A shell was used to immobilize the patient's head, and simulation X-ray radiographs or computed tomography simulation were used to determine the radiation portals and techniques. Local irradiation of the primary site was performed using parallel-opposed lateral fields in 11 patients with a total radiation dose of 60–70 Gy (median, 60 Gy). Elective bilateral neck irradiation was performed in 66 patients using parallel-opposed lateral fields with or without a matched anterior lower neck field or anterior and lateral wedge fields, with a total radiation dose of 20–50 Gy (median, 40 Gy). After the neck irradiation, the radiation to the primary lesion was boosted using a reduced parallel-opposed lateral field, with a total radiation dose of 10–40 Gy (median, 22 Gy).

Chemotherapy was administered concurrently with the RT in 16 patients for the treatment of synchronous cancers (esophageal cancer in 15, and oropharyngeal and laryngeal cancer in 1). Continuous infusions of 5-fluorouracil (5-FU; 600–1,250 mg/day; median, 1,100 mg/day) were given on the first 4 days of weeks 1 and 5 in combination with cisplatin (60–125 mg; median, 110 mg) on the first day of weeks 1 and 5 in the 15 patients with esophageal cancer, and TS-1 (100 mg/day) was successively used for 3 weeks in the 1 patient with oropharyngeal and laryngeal cancers.

Analysis

The median follow-up period was 33 months from the start of RT, ranging between 3 and 229 months. Fifteen patients were observed for less than 12 months: 3 patients died of HPC, 9 died of other cancers, 2 died of unknown reasons, and 1 was alive with another cancer. The median follow-up period for the 35 surviving patients who did not experience a recurrence was 48 months (range,10–229 months.

The overall, HPC-specific, and HPC recurrence-free survival rates and local control rate were calculated using the Kaplan-Meier method. Univariate and multivariate analyses were performed using the log-rank test and the Cox proportional hazards test. A p value of <0.05 and <0.007 was considered statistically significant in the univariate analyses and the multivariate analysis, respectively, resulting in an overall significance level of 5% (3).

Complications were assessed according to the Common Terminology Criteria for Adverse Events v3.0

RESULTS

Survival

The 5-year overall and HPC-specific survival rates for all 77 patients were 47% and 74%, respectively (Fig. 1). Thirty-nine patients died between 3.1 and 191 months (median, 15 months) after the start of RT; the causes of death were HPC in 13 patients who died 11–50 months (median, 15 months) after the start of RT, other malignancies in 16 patients (esophageal cancer in 9, lung cancer in 2, laryngeal

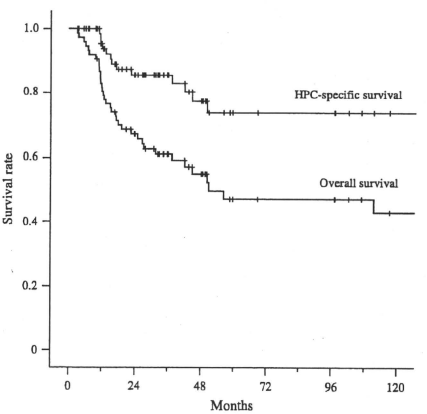

Fig. 1. Overall and hypopharyngeal cancer (HPC)–specific survival for all 77 patients.

Table 2. Overall and HPC-specific survival rates according to patient and clinical factors

Factors		*n*	Overall survival			HPC-specific survival		
			5-year (%)	Univariate *p*	Multivariate *p*	5-year (%)	Univariate *p*	Multivariate *p*
Total		77	47			74		
Sex	F	6	33			40		
	M	71	48	0.27	0.90	76	0.009	0.39
Age (y)	≤65	44	57			72		
	>65	33	34	0.12	0.042	77	0.96	0.60
HPC stage	I	42	52			85		
	II	35	43	0.43	0.18	62	0.024	0.032
HPC site	PC	12	52			59		
	PS	50	53			87		
	PW	15	27	0.052	0.058	43	0.005	0.064
RT field	Local	11	46			56		
	Locoregional	66	48	0.47	0.09	80	0.24	0.18
RT dose:	≤65	35	38			67		
primary (Gy)	>65	42	58	0.12	0.56	83	0.57	0.62
Concurrent CRT	Yes	16	23			69		
	No	61	53	0.085	0.029	74	0.92	0.22

Abbreviations: HPC = hypopharyngeal cancer; RT = radiotherapy; PC = postcricoid region; PS = pyriform fossa; PW = posterior wall; CRT = chemoradiotherapy.

cancer in 1, oropharyngeal cancer in 1, oral cancer in 1, renal cancer in 1, and malignant lymphoma in 1) who died 3.1–191 months (median, 12 months) after the start of RT, and other reasons in 10 patients (infectious pneumonia in 2, heart failure in 1, rupture of an abdominal aortic aneurysm in 1, suicide in 1, and unknown in 5) who died 3.5–57 months (median, 15 months) after the start of RT.

The relations between clinical factors and the overall and HPC-specific survival rates are shown in Table 2. Overall survival was not affected by any patient characteristics or treatment factors. Disease stage and primary site were significant factors for HPC-specific survival in the univariate analysis (disease stage, $p = 0.024$; primary site, $p = 0.005$), and the HPC-specific survival rate in patients with Stage II HPC or a primary site of PC or PW was much lower than that in patients with Stage I or a primary site of PS, but no factors were significant in the multivariate analysis.

Course of HPC

The 5-year HPC recurrence-free survival rate and local control rate with laryngeal voice preservation for all 77 patients were 57% and 70%, respectively (Fig. 2). One patient's tumor remained after RT, 1 patient was diagnosed with lymph node recurrence during RT, and 22 patients experienced disease recurrence 4–51 months (median, 10 months) after the start of RT. Thirteen (54%) of the 24 patients had local recurrences, 8 (33%) had lymph node recurrences, and 3 (13%) had local and lymph node recurrences. Distant metastases were observed in 6 patients (lung in 3, mediastinum in 2, and bone in 1) 11–49 months (median, 19 months) after the start of RT for HPC, but none of these metastases were found before local or lymph node recurrence. The relations between the clinical factors and the HPC recurrence-free survival rate and local control rate with laryngeal voice preservation are shown in Table 3. The HPC recurrence-free survival rate in patients with Stage I HPC or a locoregional RT field was significantly higher than that in patients with Stage II HPC ($p = 0.026$) or a local RT field ($p = 0.036$) in the univariate analysis, but no factors were significantly associated with HPC recurrence-free survival in the multivariate analysis. The primary site and RT field significantly affected the rate of local control with laryngeal voice preservation in the univariate analysis (primary site, $p = 0.036$; RT field, $p = 0.018$), and the local control rate in patients with irradiation of a locoregional field was significantly higher than that in patients with irradiation of a local field in the multivariate analysis ($p = 0.006$).

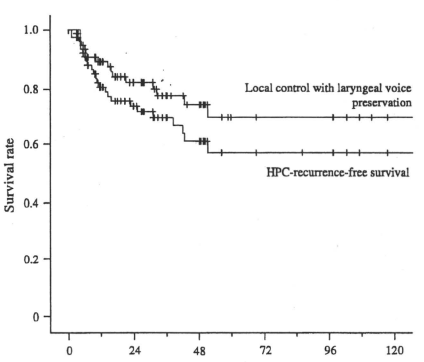

Fig. 2. Hypopharngeal cancer (HPC) recurrence-free survival and local control with laryngeal voice preservation for all 77 patients.

Table 3. HPC recurrence-free survival rate and local control rate with laryngeal voice preservation according to patient and clinical factors

Factors		n	HPC recurrence-free survival 5-year (%)	HPC recurrence-free survival Univariate p	HPC recurrence-free survival Multivariate p	Local control with voice preservation 5-year (%)	Local control with voice preservation Univariate p	Local control with voice preservation Multivariate p
Total		77	57			74		
Sex	F	6	50			67		
	M	71	57	0.28	0.90	70	0.35	0.98
Age (y)	≤65	44	49			65		
	>65	33	69	0.36	0.42	79	0.41	0.52
HPC stage	I	42	75			84		
	II	35	41	0.026	0.044	56	0.055	0.048
HPC site	PC	12	47			63		
	PS	50	62			76		
	PW	15	52	0.06	0.18	60	0.039	0.056
RT field	Local	11	38			42		
	Locoregional	66	59	0.036	0.10	73	0.018	0.006
RT dose: primary (Gy)	≤65	35	53			68		
	≥66	42	60	0.78	0.81	72	0.99	0.91
Concurrent CRT	Yes	16	56			83		
	No	61	56	0.4	0.96	68	0.5	0.52

Abbreviations: HPC = hypopharyngeal cancer; RT = radiotherapy; PC = postcricoid region; PS = pyriform fossa; PW = posterior wall; CRT = chemoradiotherapy.

Of 16 patients with local recurrence or local and lymph node recurrence, 12 underwent salvage surgery (total laryngopharyngectomy with or without neck resection in 11 and partial pharyngectomy in 1). One patient underwent chemotherapy, 2 received no treatment, and 1 patient was lost to follow-up after a local recurrence was detected. Of the 8 patients with lymph node recurrence, 6 underwent neck dissection, 1 patient underwent RT, and 1 patient received no treatment. All 3 patients who did not undergo salvage surgery died within 15 months. Only 5 patients with local recurrence and 3 patients with lymph node recurrence responded after surgery, and the 5-year overall survival rate for the 12 patients who were treated with salvage surgery was 39 % (Fig. 3). The difference in overall survival according to salvage therapy was significant ($p = 0.003$).

Of the total of 77 patients, 7 (9%) had Grade 3 or greater complications related to the treatment for HPC, and 6 of these patients experienced their complications after salvage surgery: 2 patients died as a result of arterial injury (Grade 5), 1 had a life-threatening arterial injury (Grade 4), 1 had an arterial injury requiring repair or revision (Grade 3), and 2 developed pharyngeal fistulas requiring operative intervention (Grade 3). One patient who did not have a recurrence developed otitis media with discharge (Grade 3).

Synchronous and metachronous malignancy

Of the 77 patients, 64 (83%) had synchronous or metachronous malignancies; the distribution of these malignancies is shown in Fig. 4. Forty-two had metachronous malignancies diagnosed before they underwent treatment for HPC, and 33 (79%) had esophageal cancer. These malignancies were under control at the start of treatment for HPC, but 19 of these patients had synchronous malignancies and/or metachronous malignancies after RT for HPC.

Overall, 23 patients had synchronous malignancies, 26 had metachronous malignancies after RT for HPC, and 8 had both synchronous and metachronous malignancies. The overall survival rate in the patients whose synchronous and/or metachronous malignancies were detected at an early stage (59% at 5 years) was not different from that in patients without synchronous or metachronous malignancies (48% at 5 years), but the survival rate in the patients whose synchronous or metachronous malignancies were detected at an advanced stage (17% at 5 years) was much lower than that in the patients without synchronous or metachronous malignancies

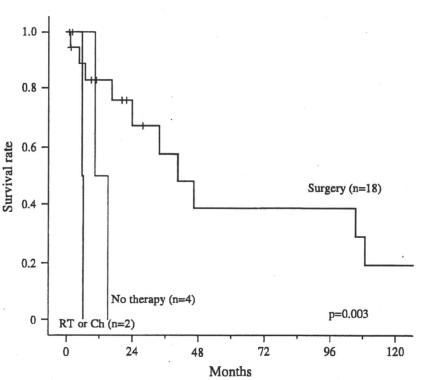

Fig. 3. Overall survival after hypopharyngeal cancer (HPC) recurrence according to salvage therapies (RT = radiotherapy; Ch = chemotherapy).

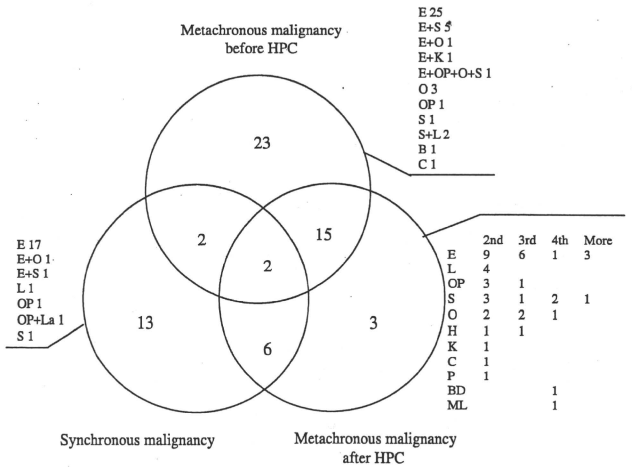

Fig. 4. Number of hypopharyngeal cancer (HPC) patients with synchronous and metachronous malignancy (E = esophagus; S = stomach; O = oral cavity; K = kidney; OP = oropharynx; B = bladder; C = colon; La = larynx; H = liver; P = prostate; BD = bile duct; ML = malignant lymphoma).

or the patients with early-stage synchronous or metachronous malignancies (Fig. 5). Advanced-stage synchronous malignancies were seen in 5 patients with esophageal cancer. All 5 patients received concurrent chemoradiotherapy, but died of their synchronous malignancies 5–13 months (median, 11 months) after the start of RT. Advanced-stage metachronous malignancies were seen in 7 of the 26 patients (lung cancer in 2, oropharyngeal cancer in 2, esophageal cancer in 1, renal cancer in 1, and prostate cancer in 1) 7.5–153 months (median, 12 months) after the start of RT for HPC. Five of these patients died of their advanced-stage metachronous malignancies (lung cancer in 2, oropharyngeal cancer in 1, esophageal cancer in 1, and renal cancer in 1).

The rates of metachronous malignancy after RT for HPC and HPC recurrence after RT, as calculated using the Kaplan-Meier method, are shown in Fig. 6. The rate of HPC recurrence increased rapidly for 2 years after RT and reached a plateau at 4 years. The rate of metachronous malignancy increased year by year after RT. The rate of second primary malignancy was 32% at 5 years and 56% at 10 years, that of third

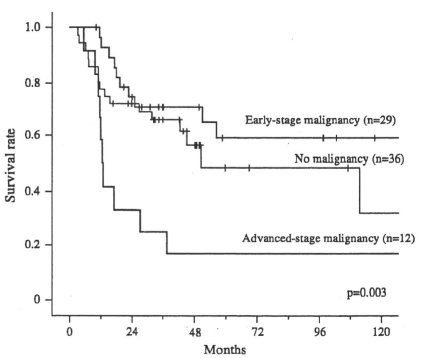

Fig. 5. Overall survival for patients with or without synchronous or metachronous malignancy after radiotherapy for hypopharyngeal cancer (HPC).

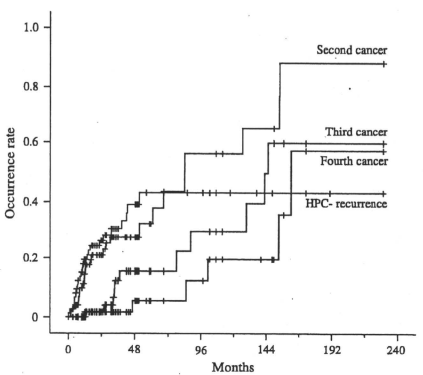

Fig. 6. Rates of hypopharyngeal recurrence and metachronous malignancy after radiotherapy.

malignancy was 15% at 5 years and 29% at 10 years, and that of fourth malignancy was 5% at 5 years and 19% at 10 years.

DISCUSSION

Radiotherapy has long been recognized as effective for early-stage squamous cell carcinoma of the hypopharynx (1, 2). However, few reports have analyzed large numbers of patients undergoing RT for early-stage HPC without lymph node metastasis, and to our knowledge, no reports have statistically analyzed predictors of survival. Concurrent chemoradiotherapy and the computed tomography–based tumor volume have been reported to be strong predictors of local control in HPC patients, including patients with advanced-stage HPC, but whether these factors affect local control or overall survival in patients with early-stage HPC remains unclear (1, 4). In our study, only the RT field significantly affected the local control rate with laryngeal voice preservation in the multivariate analysis, and a locoregional radiation field was appropriate for patients with early-stage HPC. Although disease stage affected the HPC-specific survival rate and the HPC recurrence-free survival rate and the primary site affected the HPC-specific survival rate and the local control rate in univariate analyses, these factors were not significant in a multivariate analysis. The patient and tumor characteristics had no effect on the treatment outcome of RT for early-stage HPC.

Nakamura *et al.* (1) reported the results of an analysis of 115 patients who underwent definitive RT for Stage I and Stage II HPC in a multi-institution study. Their overall and disease-specific survival rates at 5 years were 66% and 77.4%, respectively, and the progression-free survival and local control rates were 67.6% and 76.5% for patients with Stage I, and 51.5% and 62.6% for patients with Stage II at 5 years. Nakamura *et al.* (5) also reported an analysis of 43 other patients who underwent RT with or without salvage surgery for Stage I and II HPC in a single-institution study; the 5-year overall and disease-specific survival rates were 70.4% and 89.5%, respectively. Rabbani et al. (6) analyzed 123 patients with Stage T1–T2N0–N3M0 of the pyriform sinus; the 5-year overall survival, cause-specific survival, and local regional control rate for the 26 patients with T1N0M0 or T2N0M0 HPC were 58%, 85%, and 86%, respectively. In our study, the 5-year HPC-specific survival rate (74%), the HPC recurrence-free survival rate (57%), and the local control rate with laryngeal voice preservation (70%) were similar to these previously reported values, but the 5-year overall survival rate (47%) in our study was lower than the previously reported values (1, 5, 6). We suspect that the larger number of patients with synchronous and metachronous malignancies in the present study may be related to the lower rate of overall survival, compared with the results of previous reports.

The incidence of synchronous and metachronous malignancy in HPC patients has been reported to be approximately 20%, and the most common sites were the lung, the esophagus, and the urinary tract (7, 8). However, patients with early-stage primary tumors have a higher risk of developing a second primary tumor than do patients with advanced tumors because of their longer survival period (7); Nakamura et al. (1, 5) reported that the incidence of synchronous or metachronous malignancy in patients with early-stage HPC was 46.5–56.5%. In our study, 83% (64/77) of the patients had synchronous and/or metachronous malignancy and 53% (41/77) had synchronous malignancy and/or metachronous malignancy after RT for HPC; most of these malignancies were esophageal cancer. Because 54% (42/77) of these patients had a history of treatment for malignancy before the diagnosis of HPC, individual and/or environmental factors might have contributed to the formation of the multiple primary tumors in many of these patients (7). However, the overall survival rate for patients with early-stage synchronous malignancy and/or metachronous malignancy after RT for HPC was similar to that for patients without these malignancies, but the overall survival rate for patients with advanced-stage synchronous malignancy or metachronous malignancy after RT for HPC was significantly poorer. A more careful follow-up for detection of early-stage metachronous malignancy might have improved the overall survival rate in the present study.

The detection of early-stage HPC is as difficult as the detection of early-stage esophageal cancer, but the development of endoscopy has made both of these conditions detectable (9). In our study, HPC was diagnosed during gastrointestinal endoscopy examinations performed as pretreatment or follow-up examinations for other malignancies in 62% (48/77) of the patients. Recently, narrow band imaging has been reported to improve the diagnostic accuracy and sensitivity at which early-stage HPC can be detected (10). However, endoscopy techniques (*i.e.*, endoscopic laser resection) have been used only in a few institutions, and the indication for these treatments is unclear (9, 11). Although Shimizu *et al.* (9) performed endoscopic submucosal dissection in 4 patients with early-stage HPC and reported no local recurrences, no distant metastasis, and no early or late complications, Bernal-Sprekelsen *et al.* (11) performed endoscopic resection using a CO_2 laser and reported the need for a nasogastric feeding tube in 23.2% of the patients with small tumors, postoperative pneumonia in 5.7%, temporary postoperative coughing during oral intake in 28.1%, and severe swallowing difficulties in 3.8%. Thus, the factors associated with the occurrence and severity of various complications after endoscopic resection remain to be clarified (9).

In the present study, because we retrospectively analyzed the data of patients who underwent RT for early-stage HPC, we could not exclude some potential biases and study limitations from our results. However, we believe that RT is an appropriate treatment method for early-stage HPC, compared with surgical resection, because the outcome of RT was not affected by the patient or tumor characteristics in the present study, and cosmetic defects, swallowing disorders, aspiration pneumonia, and speech defects were avoided. Patients with early-stage HPC have a high risk of synchronous and metachronous malignancy, and their prognosis heavily depends on the development of such malignancies. However, if such malignancies are detected at an early

stage, patients whose HPC was treated using RT are often able to receive sufficient treatment for those malignancies, and their overall survival rate is as high as that in patients without these malignancies (1, 5, 6, 9). Patients with early-stage HPC should be carefully examined before and after the start of treatment and should be closely followed up at frequent intervals to ensure the early detection of synchronous and metachronous malignancies (7).

REFERENCES

1. Nakamura K, Shioyama Y, Kawashima M, *et al.* Multi-institutional analysis of early squamous cell carcinoma of the hypopharynx treated with radical radiotherapy. *Int J Radiat Oncol Biol Phys* 2006;65:1045–1050.
2. Foote RL. Radiotherapy alone for early-stage squamous cell carcinoma of the larynx and hypopharynx. *Int J Radiat Oncol Biol Phys* 2007;69:S31–S36.
3. Beck-Bornholdt HP, Dubben HH. Potential pitfalls in the use of *p*-values and interpretation of significance levels. *Radiother Oncol* 1994;33:171–176.
4. Shang-Wen C, Shih-Neng Y, Ji-An L, *et al.* Value of computed tomography-based tumor volume as a predictor of outcomes in hypopharyngeal cancer after treatment with definitive radiotherapy. *Laryngoscope* 2006;116: 2012–2017.
5. Nakamura K, Shioyama Y, Sasaki T, *et al.* Chemoradiation therapy with or without salvage surgery for early squamous cell carcinoma of the hypopharynx. *Int J Radiat Oncol Biol Phys* 2005;62:680–683.
6. Rabbani A, Amdur RJ, Mancuso AA, *et al.* Definitive radiotherapy for T1-T2 squamous cell carcinoma of pyriform sinus. *Int J Radiat Oncol Biol Phys* 2008;72:351–355.
7. Raghavan U, Quraishi S, Bradley PJ. Multiple primary tumors in patients diagnosed with hypopharyngeal cancer. *Otolaryngol Head Neck Surg* 2003;128:419–425.
8. Kohmura T, Hasegawa Y, Matsuura H, *et al.* Clinical analysis of multiple primary malignancies of the hypopharynx and esophagus. *Am J Otolaryngol* 2001;22:107–110.
9. Shimizu Y, Yamamoto J, Kato M, *et al.* Endoscopic submucosal dissection for treatment of early stage hypopharyngeal carcinoma. *Gastrointest Endosc* 2006;64:255–259.
10. Watanabe A, Taniguchi M, Tsujie H, *et al.* The value of narrow band imaging endoscope for early head and neck cancers. *Otolaryngol Head Neck Surg* 2008;138:446–451.
11. Bernal-Sprekelsen M, Vilaseca-Gonzalez I, Blanch-Alejandro JL, *et al.* Predictive values for aspiration after endoscopic laser resections of malignant tumors of the hypopharynx and larynx. *Head Neck* 2004;26:103–110.

Lung Cancer 70 (2010) 286–294

Contents lists available at ScienceDirect

Lung Cancer

journal homepage: www.elsevier.com/locate/lungcan

Automated assessment of malignant degree of small peripheral adenocarcinomas using volumetric CT data: Correlation with pathologic prognostic factors

Masahiro Yanagawa[a,*], Yuko Tanaka[a], Masahiko Kusumoto[b], Shunichi Watanabe[c], Ryosuke Tsuchiya[d], Osamu Honda[a], Hiromitsu Sumikawa[a], Atsuo Inoue[a], Masayoshi Inoue[d], Meinoshin Okumura[d], Noriyuki Tomiyama[a], Takeshi Johkoh[e]

[a] Department of Radiology, Osaka University Graduate School of Medicine, 2-2 Yamadaoka, Suita-city, Osaka 565-0871, Japan
[b] Department of Radiology, National Cancer Center, 5-1-1 Tukiji, Chuo-ku, Tokyo 104-0045, Japan
[c] Division of Thoracic Surgery, National Cancer Center, 5-1-1 Tukiji, Chuo-ku, Tokyo 104-0045, Japan
[d] Respiratory Surgery, Osaka University Graduate School of Medicine, 2-2 Yamadaoka, Suita-city, Osaka 565-0871, Japan
[e] Department of Radiology, Kinki Central Hospital of Mutual Aid Association of Public School Teachers, 3-1 Kurumazuka, Itami-city, Hyogo 664-8533, Japan

ARTICLE INFO

Article history:
Received 22 September 2009
Received in revised form 12 March 2010
Accepted 19 March 2010

Keywords:
Computed tomography (CT)
Volumetric CT
Small peripheral pulmonary adenocarcinoma
Ground-glass opacity
Pathological prognostic factors

ABSTRACT

Purpose: To evaluate a custom-developed software for analyzing malignant degrees of small peripheral adenocarcinomas on volumetric CT data compared to pathological prognostic factors.
Materials and methods: Forty-six adenocarcinomas with a diameter of 2 cm or less from 46 patients were included. The custom-developed software can calculate the volumetric rates of solid parts to whole nodules even though solid parts show a punctate distribution, and automatically classify nodules into the following six types according to the volumetric rates of solid parts: type 1, pure ground-glass opacity (GGO); type 2, semiconsolidation; type 3, small solid part with a GGO halo; type 4, mixed type with an area that consisted of GGO and solid parts which have air-bronchogram or show a punctate distribution; type 5, large solid part with a GGO halo; and type 6, pure solid type. The boundary between solid portion and GGO on CT was decided using two threshold selection methods for segmenting gray-scale images. A radiologist also examined two-dimensional rates of solid parts to total opacity (2D%solid) which was already confirmed with previous reports.
Results: There were good agreements between the classification determined by the software and radiologists (weighted kappa = 0.778–0.804). Multivariate logistic regression analyses showed that both 2D%solid and computer-automated classification were significantly useful in estimating lymphatic invasion ($p = 0.0007$, 0.0027), vascular invasion ($p = 0.003$, 0.012), and pleural invasion ($p = 0.021$, 0.025).
Conclusion: Using our custom-developed software, it is feasible to predict the pathological prognostic factors of small peripheral adenocarcinomas.

1. Introduction

Adenocarcinoma is the most common histopathologic subtype of lung cancer, and its incidence has been increasing [1,2]. Recent advances in CT scanning technology have enabled the detection of small pulmonary nodules, most of which are peripherally located adenocarcinoma. Such early detection using CT may alter the course of treatment of adenocarcinomas and subsequently improve the prognosis [3,4]. Although there is general consensus regarding the pathologic diagnosis of early pulmonary adenocarcinoma [5–8], the clinical and radiologic diagnosis of early adenocarcinoma with favorable prognosis remains controversial. Many reports [8,9] have demonstrated that the size of the central collapse/fibrosis and the percentage of the bronchioloalveolar carcinoma (BAC) component can be used as prognostic indicators for small lung adenocarcinomas. The BAC component is commonly detected on CT as ground-glass opacity (GGO); defined as a hazy increase in lung attenuation that does not obscure the underlying vascular markings [10]. However, there is no generally accepted method for measuring the area of GGO.

A new radiologic classification of small pulmonary adenocarcinoma on thoracic thin-section CT has already been proposed [11]. This classification, which is significantly associated with pathological prognostic factors, is based on the findings of thin-section CT

* Corresponding author at: Department of Radiology, Osaka University Graduate School of Medicine (the institution at which the work was performed), 2-2 Yamadaoka, Suita-city, Osaka 565-0871, Japan. Tel.: +81 6 879 3434; fax: +81 6 879 3439.
E-mail address: m-yanagawa@radiol.med.osaka-u.ac.jp (M. Yanagawa).

0169-5002/$ – see front matter © 2010 Elsevier Ireland Ltd. All rights reserved.
doi:10.1016/j.lungcan.2010.03.009

scans, such as the presence of solid and GGO parts, the distribution of solid parts, and the rate of solid parts to the whole nodule. However, because this classification can only be evaluated visually on CT, observers may differ in their assessment regarding the presence of solid and GGO parts. The purpose of the present study was to evaluate the ability of our custom-developed software to automatically analyze the malignant degree of small peripheral adenocarcinomas on quantitative volumetric CT data compared to pathological prognostic factors.

2. Materials and methods

2.1. Patients and diagnoses

The present study was approved by the institutional review board. Informed consent was waived for retrospective review of patient records and images. The study population consisted of consecutive patients who had undergone surgery at one hospital from January 2001 through July 2005 for primary pulmonary adenocarcinomas with a diameter of 2 cm or less. CT scans were performed in all patients before surgery. In all patients, the pulmonary nodules with a diameter of 2 cm or less in the longest diameter had areas with GGO and/or solid parts on CT, and were completely surrounded by the lung or visceral pleura at surgery. Patients who had previous adenocarcinomas in the lungs or other organs and who had undergone chemotherapy before surgery were excluded from the study. Moreover, patients were also excluded if their thin-section CT data was not available. Forty-six patients (22 men, 24 women; age range, 43–78 years; mean age, 61 years) were included in the present study.

The histopathologic diagnosis of all nodules was non-mucinous adenocarcinoma. On the basis of the histologic growth pattern, the adenocarcinomas were classified into the following three subtypes: localized BAC ($n = 16$), adenocarcinoma with BAC component ($n = 29$), and adenocarcinoma without BAC component ($n = 1$). The 16 cases of BAC included 3 cases associated with atypical adenomatous hyperplasia.

2.2. Acquisition of thin-section CT images

Chest CT scans were conducted using a 4-detector row LightSpeed QXi Scanner (General Electric Medical Systems, Milwaukee, WI, USA), an 8-detector row LightSpeed Ultra Scanner (GE Healthcare Technologies, Milwaukee, WI, USA), or a 4-detector row Aquilion V-detector Scanner (Toshiba Medical Systems, Tokyo, Japan). The parameters used for the scans depended on the indication: collimation was 0.5 or 1.25 mm, pitch was 0.625–1.5, the rotation time was 0.5–0.8 s per rotation, exposure parameters were 120 kV and 200 mA, and the field of view was 200 mm. All image data were reconstructed with a high spatial frequency algorithm at a 0.5- or 1.25-mm interval. All CT scans were displayed on a monitor at lung window settings (level, −700 Hounsfield units [HU]; width, 1200 HU).

2.3. Development of software

2.3.1. Definition of GGO, semiconsolidation, and solid component

Radiologic classifications of small pulmonary adenocarcinomas were classified into six subgroups (types 1–6) according to malignant degree of the tumor, and were in agreement with a previous report [11] (Table 1). Generally, opacity of peripheral adenocarcinomas on CT can be visually broken down into three parts, such as GGO, semiconsolidation, and solid part. GGO was defined as an area exhibiting a slight, homogeneous increase in density, which did not obscure underlying vascular markings. Semiconsolidation was defined as an area exhibiting an intermediate homogeneous increase in density, which did not obscure underlying vascular markings. The solid part was defined as an area of increased opacification that completely obscured underlying vascular markings. Prior to the present study, we determined threshold CT values between GGO and semiconsolidation and between semiconsolidation and solid parts in an additional six cases with adenocarcinomas, other than those in the present study, in order to automatically segment the three parts using our custom-developed software. By consensus, two radiologists assessed whether the tumor was GGO, semiconsolidation, or solid part from CT images of these additional six adenocarcinomas.

Two automatic threshold selection methods for segmenting gray-level images were used in the present study, 1: Method-1, Otsu's method [12], and 2: Method-2, Kittler's method [13]. Method-1 is a nonparametric and unsupervised method of automatic threshold selection for picture segmentation [12]. This simple method enables the division of gray images into two separate images through the selection of a threshold from gray-level histograms. Utilizing only the zeroth- and the first-order cumulative moments of the gray-level histogram, extending this method to multithreshold problems is straightforward. Method-2 is based on "minimum error thresh-holding" [13]. A computationally efficient solution to the problem of minimum error thresholding is derived under the assumption that both object and pixel gray-level values are normally distributed. The thresholds between GGO and semiconsolidation were −547 HU using Method-1 and −534 HU using Method-2; those between semiconsolidation and solid part were −291 HU using Method-1 and −188 HU using Method-2 (Figs. 1 and 2).

2.3.2. Decision of cut-off value of rate of solid part to total tumor (% solid) for the three-dimensional classification of tumors

According to radiologic classifications used in the present study (Table 1), the two-dimensional % solid (2D%solid) of type 3 or 4 was less than 50%, and 2D%solid of type 5 was 50% or more on transverse CT images [11]. In expanding the classifications on two-dimensional images to those on three-dimensional images, the cut-off value of three-dimensional % solid (3D%solid) between types 3 and 5 was 35.4% [$=(0.5)^{3/2} \times 100\%$].

In contrast, nodules from a previous experiment conducted using ten adenocarcinomas, different from those used in the present study, were classified based on visual assessment, as only

Table 1
Radiologic classifications of small pulmonary adenocarcinomas on CT images.

Classification	Radiologic Findings
Type 1	Pure GGO
Type 2	Semiconsolidation (an area of an intermediate homogeneous increase in density, which did not obscure underlying vascular markings)
Type 3	Small solid part with a GGO halo (an area that consisted of a solid part and a surrounding GGO halo; the area of solid part should be less than 50% on transverse CT image)
Type 4	Mixed type (an area that consisted of GGO and solid parts that have air-bronchogram or that show a punctate distribution; the area of solid part should be less than 50% on transverse CT image)
Type 5	Large solid part with a GGO halo (the area of solid part should be 50% or more on transverse CT image)
Type 6	Pure solid type (a nodule visually appeared to consist of only solid components)

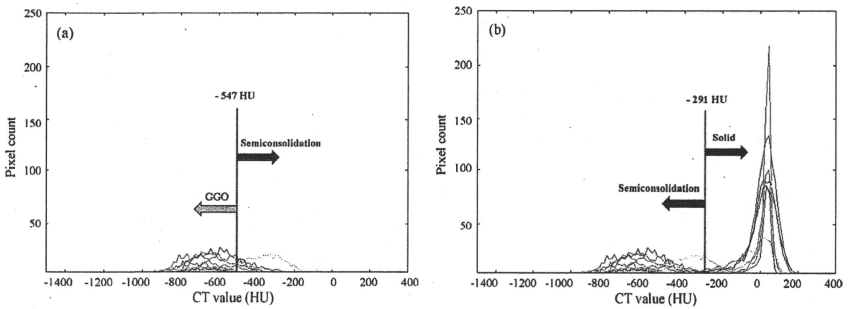

Fig. 1. (1) Threshold selection methods for segmenting gray-level images (Method-1, Otsu's method): the threshold between GGO and semiconsolidation. The gray-level histogram was generated using cases of type 1 (GGO) and 2 (semiconsolidation). The threshold (red line) between GGO and semiconsolidation was −547 HU using Method-1. (2) Threshold selection methods for segmenting gray-level images (Method-1, Otsu's method): the threshold between semiconsolidation and solid. The gray-level histogram was generated using cases of type 2 (semiconsolidation) and 6 (solid). The threshold (blue line) between semiconsolidation and solid was −291 HU using Method-1.

Table 2
Modified radiologic classifications on 3D-CT images.

Classification	Radiologic findings by Method-1 or Method-2
Type 1	Tumor with a CT value less than *x* HU.
Type 2	Tumor with a CT value from *x* HU to *y* HU.
Types 3–6	Tumor including a solid part with a CT value more than *y* HU.
Type 3	The volume rate of solid part should be less than 35.4%.
Type 4	The volume rate of solid part should be less than 35.4%. Solid parts have air-bronchogram or show a punctate distribution.
Type 5	The volume rate of solid part should be from 35.4 to 71.5%.
Type 6	The volume rate of solid part should be greater than 71.5%.

Method-1 (Otsu's method): $x = -547$, $y = -291$.
Method-2 (Kittler's method): $x = -534$, $y = -188$.

solid part (type 6). This experiment revealed that 2D%solid on transverse CT images calculated using Method-1 or Method-2 was equivalent to about 80%. Therefore, the cut-off value of 3D%solid between types 5 and 6 was 71.5% [$=(0.8)^{3/2} \times 100\%$]. The modified radiologic classifications on 3D images are summarized in Table 2.

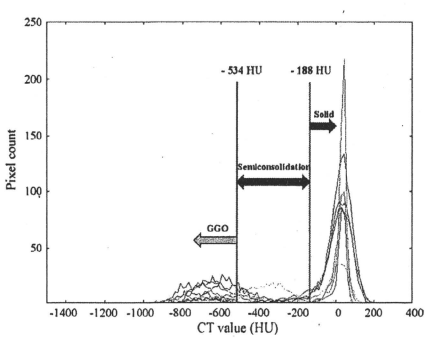

Fig. 2. Threshold selection methods for segmenting gray-level images (Method-2, Kittler's method): the thresholds among GGO, semiconsolidation and solid. Method-2 is based on "minimum error thresh-holding", which can decide more than two thresholds. The gray-level histogram was generated using cases of type 1 (GGO), 2 (semiconsolidation) and 6 (solid). The threshold (red line) between GGO and semiconsolidation was −534 HU and that (blue line) between semiconsolidation and solid was −188 HU using Method-2.

2.3.3. *Outline of custom-developed software*

Our software was developed using Microsoft Visual C++ 6.0 (Microsoft Corporation, Redmond, WA, USA) on a commercially available personal computer. It was a plug-in for the software used to segment the nodules on volumetric CT data, and used the following algorithm. First, by manually highlighting the boundary between the tumor and normal lung parenchyma on every CT slice, each volume of GGO, semiconsolidation, and solid part included in the highlighted area is automatically segmented. Next, the 3D%solid of the tumor is also automatically calculated. Finally, the tumors are automatically classified into the subgroups (types 1–6) (Fig. 3). Computer-automated classification according to malignant degree of the tumor on 3D-CT images is summarized in Fig. 4.

2.4. *Image analysis*

Three independent chest radiologists (with 8, 20 and 21 years of experience, respectively) visually classified tumors into the six subgroups (types 1–6) according to a previous report [11]. Final visual classification of the subgroup was decided by consensus.

The chest radiologist with 8 years of experience also manually examined 2D%solid on the maximum cross-section of the CT images directly on the monitor using a caliper, because the utility of a prognostic prediction using 2D%solid on CT images was already confirmed with previous reports [14].

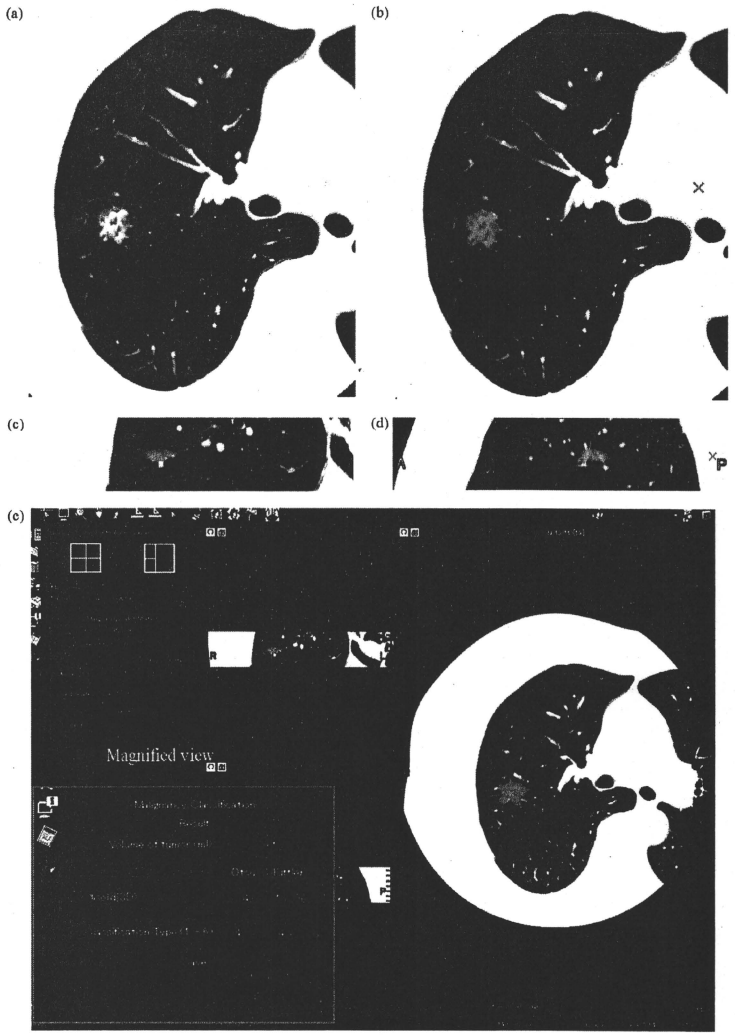

Fig. 3. A case of type 4 tumor in a 68-year-old woman. Axial CT image (a) shows a tumor with an area that consisted of GGO and solid parts. The green areas ((b) axial CT image, (c) coronal CT image, and (d) sagittal CT image) show an extracted tumor. Overall view of our software is shown by (e). Green frame is a magnified view of red frame. Our software indicates a tumor volume of 9.13 ml: 3D%solid using Method-1 is 30.493% and using Method-2 (Kittler's method) is 15.696%. Our software classified this tumor as type 4 (mixed type with an area that consisted of GGO and solid parts that have air-bronchogram or that show a punctate distribution).

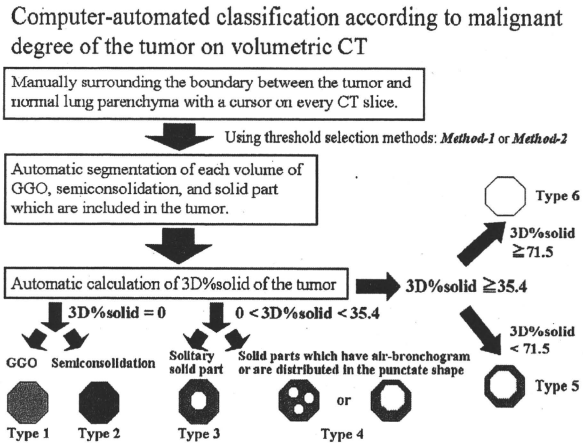

Fig. 4. Flow chart of computer-automated classification according to malignant degree of the tumor on volumetric CT.

This radiologist obtained the following information from the thin-slice CT images: the maximum dimension of tumor using a pulmonary window level setting (level, 600 HU; width, 1600 HU), the largest dimension of the perpendicular axis using a pulmonary window level setting, the maximum dimension of tumor using a mediastinal window level setting (level, 40 HU; width, 400 HU), and the largest dimension of the perpendicular axis using a mediastinal window level setting.

Highlighting of the boundary between the tumor and normal lung parenchyma using our software was conducted by two independent chest radiologists (4 and 8 years of experience). After discussion, the data from one experienced chest radiologist (the same radiologist who measured 2D%solid on CT) were used for analysis.

We evaluated three matters (vascular, lymphatic and pleural invasion) as pathological prognostic factors and examined the correlation of these three prognostic factors with the four explanatory variables: the visual classification of the subgroup; the classification using Method-1; the classification using Method-2 and manually measured 2D%solid.

2.5. Statistical analysis

Statistical analysis was performed using commercially available software (MedCalc Version 8.0.0.1, Frank Schoonjans, Mariakerke, Belgium). Inter-observer agreements of highlighted boundaries between tumors and normal lung parenchyma were assessed by Bland and Altman's method [15]. Agreements between visual and computer-automated classification were evaluated using the weighted κ statistic and classified as poor ($\kappa = 0.00–0.20$), fair ($\kappa = 0.21–0.40$), moderate ($\kappa = 0.41–0.60$), good ($\kappa = 0.61–0.80$), or excellent ($\kappa = 0.81–1.00$). Univariate and multivariate analyses were performed by logistic regression analysis. Forward and backward stepwise procedures were used to determine the combination of factors that were essential in predicting prognosis. A p value < 0.05 was considered to indicate significant difference.

3. Results

3.1. Inter-observer agreements

Inter-observer agreement between the two observers that manually highlighted the boundary between the tumor and normal lung parenchyma (mean bias ± 1.96 standard deviations) was −2.2 ± 9.5 mm (Fig. 5).

3.2. Agreements between visual classification and computer-automated classification

The visual classification by radiologists was as follows: type 1 (11/46 cases, 24%), type 2 (2/46, 4%), type 3 (4/46, 9%), type 4 (9/46, 20%), type 5 (13/46, 28%) and type 6 (7/46, 15%). The agreement between visual and computer-automated classification are shown in Table 3. Overall concordance between visual classification and classification using Method-1 was 32 (70%) of 46 tumors (weighted kappa = 0.799). Overall concordance between visual classification and the classification using Method-2 was 29 (63%) of 46 tumors (weighted kappa = 0.758).

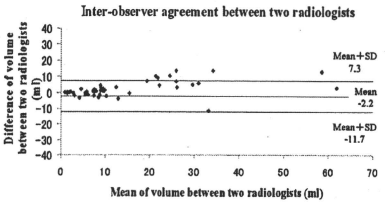

Fig. 5. Bland–Altman plot of inter-observer agreement between two radiologists.

Table 3
The agreement between visual and computer-automated classification (Method-1 or Method-2).

	Visual classification						Total
	Type 1	Type 2	Type 3	Type 4	Type 5	Type 6	
Method-1 (Otsu's method)							
Type 1	9	1	0	0	0	0	10
Type 2	1	0	0	0	0	0	1
Type 3	0	1	2	2	1	0	6
Type 4	1	0	1	5	0	0	7
Type 5	0	0	1	2	11	2	16
Type 6	0	0	0	0	1	5	6
Total	11	2	4	9	13	7	46
Weighted kappa value				0.799			
Method-2 (Kittler's method)							
Type 1	10	2	1	0	0	0	13
Type 2	0	0	0	1	0	0	1
Type 3	1	0	0	3	2	0	6
Type 4	0	0	3	5	1	0	9
Type 5	0	0	0	0	10	3	13
Type 6	0	0	0	0	0	4	4
Total	11	2	4	9	13	7	46
Weighted kappa value				0.758			

3.3. *Manually measured 2D%solid on the maximum cross-section of CT*

Manually measured 2D%solid (mean ± standard deviation) according to the visual classification is shown in Table 4. In the case of solid parts that have air-bronchogram or that show a punctate distribution (type 4), the radiologist made all possible efforts to measure the 2D%solid of tumors.

3.4. *Pathologic characteristic according to classification of tumors*

Pathologic characteristics in small pulmonary adenocarcinomas according to visual and computer-automated classification are summarized in Table 5. In both localized BAC ($n = 16$) and adenocarcinoma without BAC component ($n = 1$), there were no differences in distribution of pathologic characteristics among visual classification, classification using Method-1, and classification using Method-2. In adenocarcinoma with BAC component ($n = 29$), there were differences in distribution of pathologic characteristics among these three types of classifications. Univariate and multivariate logistic regression analyses are summarized in Tables 6.1 and 6.2. Univariate logistic regression analyses showed that classification using Method-1 and manually measured 2D%solid were both significantly useful in estimating all three pathological prognostic factors: lymphatic invasion ($p = 0.01$, 0.0007), vascular invasion ($p = 0.017$, 0.003) and pleural invasion ($p = 0.03$, 0.046). Multivariate logistic regression analyses also demonstrated that classification using Method-1 and manually measured 2D%solid were both significantly useful in estimating lymphatic invasion ($p = 0.0027$, 0.0007), vascular invasion ($p = 0.012$, 0.003) and pleural invasion ($p = 0.025$, 0.021).

Table 4
Manually measured two-dimensional % solid (2D%solid) according to visual classification.

Visual classification	2D%solid (mean ± SD)
Type 1 ($n = 11$)	0 ± 0
Type 2 ($n = 2$)	0 ± 0
Type 3 ($n = 4$)	0.182 ± 0.149
Type 4 ($n = 9$)	0.055 ± 0.072
Type 5 ($n = 13$)	0.444 ± 0.191
Type 6 ($n = 7$)	0.948 ± 0.135
Total ($n = 46$)	0.297 ± 0.354

4. Discussion

The present study demonstrates that our custom-developed software is useful for predicting lymphatic invasion, vascular invasion and pleural invasion in small peripheral adenocarcinomas. Even though pulmonary nodules show various CT patterns (GGO, semiconsolidation, part-solid, and pure solid) and have solid parts with a punctate distribution, predicting the pathological prognostic factors of them on CT images is feasible using our custom-developed software.

The prognosis of pulmonary adenocarcinoma with a larger area of GGO on thin-section CT images is much better than that of pulmonary adenocarcinoma of solid type on CT regardless of its maximal tumor dimension [4,16–21]. The extent of GGO is one of the most important prognostic factors. In fact, there were differences in distribution of pathologic characteristics among visual classification, classification using Method-1, and classification using Method-2 in adenocarcinomas with BAC component which is commonly detected on CT as GGO (Table 5). Many reports have demonstrated that manually measured 2D%solid on thin-section CT images was useful for predicting the prognostic outcome of small pulmonary adenocarcinomas [4,14,17–19,22–26]. However, the reproducibility of manual measurements is poor in evaluating small nodules [27,28]. Furthermore, malignant nodules do not always grow symmetrically, and tumors are often a heterogeneous mixture of GGO and solid parts. GGO can only be evaluated visually on CT images because there is no quantitative definition of GGO. Therefore, it is difficult to accurately measure the area of GGO and solid parts that have air-bronchogram or that show a punctate distribution, and considerable disagreement among radiologists on the diagnosis can arise.

Recent advances in diagnostic modalities have enabled the detection of increasingly smaller pulmonary adenocarcinomas with or without GGO in elderly patients. A suitable surgical approach that achieves the most benefit for these patients must be considered, and limited surgical resection has the benefit of preserving the postoperative quality of life without impairment of respiratory function [29]. Some reports [30,31] have suggested that

Table 5
Pathologic characteristics in small pulmonary adenocarcinomas according to visual and computer-automated classification.

Histopathologic diagnosis	Visual classification	Numbers of invasive tumors			Classification using Method-1 (Otsu)	Numbers of invasive tumors			Classification using Method-2 (Kittler)	Numbers of invasive tumors		
		LI	VI	PI		LI	VI	PI		LI	VI	PI
Localized BAC $n=16$	Type 1 ($n=9$)	0	1	0	Type 1 ($n=8$)	0	1	0	Type 1 ($n=11$)	0	1	0
	Type 2 ($n=2$)	0	0	0	Type 2 ($n=1$)	0	0	0	Type 2 ($n=1$)	0	0	0
	Type 3 ($n=1$)	0	0	0	Type 3 ($n=3$)	0	0	0	Type 3 ($n=2$)	0	0	0
	Type 4 ($n=3$)	0	0	0	Type 4 ($n=3$)	0	0	0	Type 4 ($n=1$)	0	0	0
	Type 5 ($n=1$)	0	0	0	Type 5 ($n=1$)	0	0	0	Type 5 ($n=1$)	0	0	0
	Type 6 ($n=0$)	0	0	0	Type 6 ($n=0$)	0	0	0	Type 6 ($n=0$)	0	0	0
Adenocarcinoma with BAC component $n=29$	Type 1 ($n=2$)	0	0	0	Type 1 ($n=2$)	0	0	0	Type 1 ($n=2$)	0	0	0
	Type 2 ($n=0$)	0	0	0	Type 2 ($n=0$)	0	0	0	Type 2 ($n=0$)	0	0	0
	Type 3 ($n=3$)	1	1	1	Type 3 ($n=3$)	1	0	0	Type 3 ($n=4$)	2	2	0
	Type 4 ($n=6$)	3	2	0	Type 4 ($n=4$)	1	1	0	Type 4 ($n=8$)	3	2	1
	Type 5 ($n=11$)	6	4	1	Type 5 ($n=14$)	9	6	1	Type 5 ($n=11$)	8	5	2
	Type 6 ($n=7$)	7	5	2	Type 6 ($n=6$)	6	5	3	Type 6 ($n=4$)	4	3	1
Adenocarcinoma without BAC component $n=1$	Type 1 ($n=0$)	0	0	0	Type 1 ($n=0$)	0	0	0	Type 1 ($n=0$)	0	0	0
	Type 2 ($n=0$)	0	0	0	Type 2 ($n=0$)	0	0	0	Type 2 ($n=0$)	0	0	0
	Type 3 ($n=0$)	0	0	0	Type 3 ($n=0$)	0	0	0	Type 3 ($n=0$)	0	0	0
	Type 4 ($n=0$)	0	0	0	Type 4 ($n=0$)	0	0	0	Type 4 ($n=0$)	0	0	0
	Type 5 ($n=1$)	1	0	0	Type 5 ($n=1$)	1	0	0	Type 5 ($n=1$)	1	0	0
	Type 6 ($n=0$)	0	0	0	Type 6 ($n=0$)	0	0	0	Type 6 ($n=0$)	0	0	0
Total $n=46$	Type 1 ($n=11$)	0	1	0	Type 1 ($n=10$)	0	1	0	Type 1 ($n=13$)	0	1	0
	Type 2 ($n=2$)	0	0	0	Type 2 ($n=1$)	0	0	0	Type 2 ($n=1$)	0	0	0
	Type 3 ($n=4$)	1	1	1	Type 3 ($n=6$)	1	0	0	Type 3 ($n=6$)	2	2	0
	Type 4 ($n=9$)	3	2	0	Type 4 ($n=7$)	1	1	0	Type 4 ($n=9$)	3	2	1
	Type 5 ($n=13$)	7	4	1	Type 5 ($n=16$)	10	6	1	Type 5 ($n=13$)	9	5	2
	Type 6 ($n=7$)	7	5	2	Type 6 ($n=6$)	6	5	3	Type 6 ($n=4$)	4	3	1

LI, lymphatic invasion; VI, vascular invasion; PI, pleural invasion.

Table 6.1
Univariate logistic regression analyses (forward and backward stepwise procedure).

Variable	Odds ratio	95% Confidence Interval	p Value
Lymphatic invasion			
Visual classification	3.99	1.6565–9.6293	0.002*
Classification using the Method-1 (Otsu's method)	12.36	1.7745–86.0956	0.01*
Classification using the Method-2 (Kittler's method)	3.7	1.6176–8.4713	0.002*
Manually measured two-dimensional % solid (2D%solid)	269.91	10.5143–6929.15	0.0007*
Vascular invasion			
Visual classification	1.83	1.0963–3.0457	0.02*
Classification using the Method-1 (Otsu's method)	2.31	1.1593–4.5964	0.017*
Classification using the Method-2 (Kittler's method)	1.73	1.0491–2.8598	0.03*
Manually measured two-dimensional % solid (2D%solid)	23.6	2.9398–189.5308	0.003*
Pleural invasion			
Visual classification	1.91	0.7553–4.8530	0.17
Classification using the Method-1 (Otsu's method)	13.58	1.2144–151.9337	0.03*
Classification using the Method-2 (Kittler's method)	2.52	0.7982–7.9872	0.11
Manually measured two-dimensional % solid (2D%solid)	9.5	1.0377–86.9719	0.046*

* Significant difference.

Table 6.2
Multivariate logistic regression analyses (forward and backward stepwise procedure).

Variable	Odds ratio	95% Confidence Interval	p Value
Lymphatic invasion			
Classification using the Method-1 (Otsu's method)	2.4	1.8249–17.7953	0.0027*
Manually measured two-dimensional % solid (2D%solid)	269.9	10.5143–17.7953	0.0007*
Vascular invasion			
Classification using the Method-1 (Otsu's method)	2.4	1.2176–4.8913	0.012*
Manually measured two-dimensional % solid (2D%solid)	23.6	2.9398–189.5308	0.003*
Pleural invasion			
Classification using the Method-1 (Otsu's method)	16.3	1.3991–189.9486	0.025*
Manually measured two-dimensional % solid (2D%solid)	54.6	1.08392–1621.0114	0.021*

* Significant difference.

segmental resection for small-sized lung cancer may be acceptable for patients with a tumor 2.0 cm or less in diameter (without nodal involvement), and that a peripherally located lung cancer with no lymph node metastasis might be the optimal indication for a more limited anatomic resection. Consequently, in current clinical settings, where limited surgical resection is desirable, the preoperative diagnosis of the invasiveness of a lung cancer becomes increasingly crucial for deciding the operative procedure. Therefore, in our study, in order to obtain an objective and quantitative assessment tool, we developed software that cannot only calculate 3D%solid of tumors including GGO area, but also automatically classify nodules according to the volumetric rates of the solid parts.

Automatic segmentation using the custom-developed software may enable high reproducibility during image assessment regardless of experience. In fact, commercially available software that can segment pulmonary nodules with GGO is already available. A previous study demonstrated that volumetric analysis is a reproducible and promising quantitative method using this commercially available software but that the correlation between the histological classification and the 3D%solid of tumors was no better when obtained using the software than when using manual measurements [32]. Although the automatic segmentation ability of our software can be improved, this software using Method-1 was as useful for predicting lymphatic invasion, vascular invasion and pleural invasion as the prognostic prediction using 2D%solid; in agreement with previous reports.

One of the important purposes of our study is to determine, as objectively as possible, the indication for limited surgical resection for lung adenocarcinomas by using our custom-developed software. Using visual classification, Suzuki et al. [11] demonstrated that types 1–4 were thought to be "minimally invasive" adenocarcinoma and that types 5 and 6 were considered to exhibit a "solid" course with higher possibility of lymph node metastases than types 1–4. If a tumor were classified as being types 1–4, the patient would be a candidate for limited surgical resection; whereas a type 5 or 6 tumor warrants major lung resection with systematic lymph node dissection necessarily. In classification using Method-1, useful for the prognostic prediction in the present study, types 5 and 6 tended to be more invasive than types 1–4 (Table 5): lymphatic invasion (types 1–4 vs. types 5 and 6), 2/24 (8%) vs. 16/22 (72%); vascular invasion, 2/24 (8%) vs. 11/22 (50%); and pleural invasion, 0/24 (0%) vs. 4/22 (18%).

However, six classifications proposed in our study are thought to remain important in order for the surgeon to plan for the management of peripheral lung cancer. In general, the progress of most small nodules that have been difficult to diagnose using CT has occurred over several years; with surgery only being indicated when tumors showed an increase in size on CT images. For instance, type 1 tumors (pure GGO) and type 2 tumors (semiconsolidation) show no solid parts on CT images. Most of the type 1 tumors are BAC, and are often indolent tumors. In contrast, type 2 tumors tend to be adenocarcinoma with pathologically invasive foci and grow in size. Concerning the surgical indications for tumors without solid parts, surgeons usually just monitor type 1 tumors without surgical interventions if the radiologic maximal tumor dimension is unchanged, and do not monitor type 2 tumors [11]. Thus, the clinical strategy depends on the six classifications, and the preoperative use of our custom-developed software will assist in determining a suitable operative method: limited surgical resection for tumors classified as types 1–4 and major lung resection for tumors classified as type 5 or 6.

There were several limitations in the present study. First, the number of patients was small for both the clinical evaluation and examination of the threshold of CT value between GGO and

semiconsolidation and between semiconsolidation and solid part. Subsequent analysis using a greater number of lung tumors is required. Second, in the image analysis, two independent readers were the minimum for this study with the current design. It might have been better for more independent readers to analyze image. Third, solid parts including vessels were calculated in our study, and may have introduced some bias into our results. In order to remove unnecessary vessels, this software will need to be upgraded by using "line filtering" [33], which enhances curvilinear structures, such as vessels and bronchi, in 3D medical images. Forth, although our software enabled automatic classification according to the malignant degree of small peripheral adenocarcinomas by automatically measuring 3D%solid of tumors, the initial highlighting of the boundary between the tumor and normal lung parenchyma was performed manually. The software is currently being upgraded to automate this procedure, which, in turn, may generate more objective results. Finally, our results should have been compared to the volumetric distribution of tumors in pathologic specimens, but postoperative collapse of the lung would have made accurate comparisons difficult.

In conclusion, predicting the pathological prognostic factors of small peripheral adenocarcinomas on three-dimensional CT images is feasible using our custom-developed software for evaluating their degree of malignancy. The application of this software will assist in deciding the future treatment strategies for small-sized adenocarcinoma of the lung following improvements in the filtering and automated segmentation feature.

Conflict of interest

No authors indicated potential conflicts of interest.

References

[1] Auerbach O, Garfinkel L. The changing pattern of the lung carcinoma. Cancer 1991;68:1973–7.

[2] Barsky SH, Cameron R, Osann KE, Tomita D, Holmes EC. Rising incidence of bronchioloalveolar lung carcinoma and its unique clinicopathologic features. Cancer 1994;73:1163–70.

[3] Henschke CI, McCauley DI, Yankelevitz DF, Naidich DP, McGuinness G, Miettinen OS, et al. Early lung cancer action project: overall design and findings from baseline screening. Lancet 1999;354:99–105.

[4] Aoki T, Tomoda Y, Watanabe H, Nakata H, kasai T, Hashimoto H, et al. Peripheral lung adenocarcinoma: correlation of thin-section CT findings with histologic prognostic factors and survival. Radiology 2001;220:803–9.

[5] Shimosato Y, Suzuki A, Hashimoto T, Nishiwaki Y, Kodama T, Yoneyama T, et al. Prognostic implications of fibrotic focus (scar) in small peripheral lung cancers. Am J Surg Pathol 1980;4:365–73.

[6] Noguchi M, Morikawa A, Kawasaki M, Matsuno Y, Yamada T, Hirohashi S, et al. Small adenocarcinoma of the lung. Histologic characteristics and prognosis. Cancer 1995;75:2844–52.

[7] Yokose T, Suzuki K, Nagai K, Nishiwaki Y, Sasaki S, Ochiai A. Favorable and unfavorable morphological prognostic factors in peripheral adenocarcinoma of the lung 3 cm or less in diameter. Lung Cancer 2000;29:179–88.

[8] Suzuki K, Yokose T, Yoshida J, Nishimura M, Takahashi K, Nagai K, et al. Prognostic significance of the size of central fibrosis in peripheral adenocarcinoma of the lung. Ann Thorac Surg 2000;69:893–7.

[9] Kurokawa T, Matsuno Y, Noguchi M, Mizuno S, Shimosato Y. Surgically curable "early" adenocarcinoma in the periphery of the lung. Am J Surg Pathol 1994;18:431–8.

[10] Austin JHM, Muller NL, Friedman PJ, Hansell DM, Naidich DP, Remy-Jardin M. Glossary of terms for CT of the lung: recommendations of the Nomenclature Committee of the Fleischner Society. Radiology 1996;200:327–31.

[11] Suzuki K, Kusumoto M, Watanabe S, Tsuchiya R, Asamura H. Radiologic classification of small adenocarcinoma of the lung: radiologic-pathologic correlation and its prognostic impact. Ann Thorac Surg 2006;81:413–20.

[12] Otsu N. A threshold selection method from gray-level histograms. IEEE Trans Syst Man Cybern 1979;SMC-9(1):62–6.

[13] Kittler J, Illingworth J. Minimum error thresholding. Pattern Recog 1986;19(1):41–7.

[14] Shimizu K, Yamada K, Saito H, Noda K, Nakayama H, Kameda Y, et al. Surgically curable peripheral lung carcinoma: correlation of thin-section CT findings with histologic prognostic factors and survival. Chest 2005;127:871–8.

[15] Bland JM, Altman DG. Statistical methods for assessing agreement between two methods of clinical measurement. Lancet 1986;1:307–10.

[16] Jang HJ, Lee KS, Kwon OJ, Rhee CH, Shim YM, Han J. Bronchioloalveolar carcinoma: focal area of ground-glass attenuation at thin-section CT as an early sign. Radiology 1996;199:485–8.

[17] Kodama K, Higashiyama M, Yokouchi H, Takami K, Kuriyama K, Mano M, et al. Prognostic value of ground-glass opacity found in small lung adenocarcinoma on high-resolution CT scanning. Lung Cancer 2001;33:17–25.

[18] Kim EA, Johkoh T, Lee KS, Han J, Fujimoto K, Sadohara J, et al. Quantification of ground glass opacity on high-resolution CT of small peripheral adenocarcinoma of the lung: pathologic and prognostic implications. AJR Am J Roentgenol 2001;177:1417–22.

[19] Ohde Y, Nagai K, Yoshida J, Nishimura M, Takahashi K, Suzuki K, et al. The proportion of consolidation to ground-glass opacity on high resolution CT is a good predictor for distinguishing the population of non-invasive peripheral adenocarcinoma. Lung Cancer 2003;42:303–10.

[20] Suzuki K, Asamura H, Kusumoto M, Kondo H, Tsuchiya R. "Early" peripheral lung cancer: prognostic significance of ground glass opacity on thin-section computed tomographic scan. Ann Thorac Surg 2002;74:1635–9.

[21] Yanagawa M, Kuriyama K, Kunitomi Y, Tomiyama N, Honda O, Sumikawa H, et al. One-dimensional quantitative evaluation of peripheral lung adenocarcinoma with or without ground-glass opacity on thin-section CT images using profile curves. Br J Radiol 2009;82(979):532–40.

[22] Kuriyama K, Seto M, Kasugai T, Higashiyama M, Kido S, Sawai Y, et al. Ground-glass opacity on thin-section CT: value in differentiating subtypes of adenocarcinoma of the lung. AJR Am J Roentgenol 1999;173:465–9.

[23] Takashima S, Maruyama Y, Hasegawa M, Yamada T, Honda T, Kadoya M, et al. Prognostic significance of high-resolution CT findings in small peripheral adenocarcinoma of the lung: a retrospective study on 64 patients. Lung Cancer 2002;36:289–95.

[24] Aoki T, Nakata H, Watanabe H, Nakamura K, Kasai T, Hashimoto H, et al. Evolution of peripheral lung adenocarcinomas: CT findings correlated with histology and tumor doubling time. AJR Am J Roentgenol 2000;174:763–8.

[25] Okada M, Nishio W, Sakamoto T, Uchino K, Tsubota N. Discrepancy of computed tomographic image between lung and mediastinal windows as a prognostic implication in small lung adenocarcinoma. Ann Thorac Surg 2003;76:1828–32.

[26] Matsuguma H, Nakahara R, Anraku M, Kondo T, Tsuura Y, Kamiyama Y, et al. Objective definition and measurement method of ground-glass opacity for planning limited resection in patients with clinical stage IA adenocarcinoma of the lung. Eur J Cardiothorac Surg 2004;25:1102–6.

[27] Revel MP, Bissery A, Bienvenu M, Aycard L, Lefort C, Frija G. Are two-dimensional CT measurements of small noncalcified pulmonary nodules reliable? Radiology 2004;231:453–8.

[28] Jennings SG, Winer-Muram HT, Tarver RD, Farber MO. Lung tumor growth: assessment with CT—comparison of diameter and cross-sectional area with volume measurements. Radiology 2004;231:866–71.

[29] Stair JM, Womble J, Schaefer RF, Read RC. Segmental pulmonary resection for cancer. Am J Surg 1985;150:659–64.

[30] Yoshikawa K, Tsubota N, Kodama K, Ayabe H, Taki T, Mori T. Prospective study of extended segmentectomy for small lung tumors: the final report. Ann Thorac Surg 2002;73:1055–8.

[31] Okada M, Nishio W, Sakamoto T, Uchino K, Yuki T, Nakagawa A, et al. Effect of tumor size on prognosis in patients with non-small cell lung cancer: the role of segmentectomy as a type of lesser resection. J Thorac Cardiovasc Surg 2005;129:87–93.

[32] Sumikawa H, Johkoh T, Nagareda T, Sekiguchi J, Matsuo K, Fujita Y, et al. Pulmonary adenocarcinomas with ground-glass attenuation on thin-section CT: quantification by three-dimensional image analyzing method. Eur J Radiol 2008;65(January (1)):104–11.

[33] Sato Y, Nakajima S, Shiraga N, Atsumi H, Yoshida S, Koller T, et al. Three-dimensional multi-scale line filter for segmentation and visualization of curvilinear structures in medical images. Med Image Anal 1998;2:143–68.